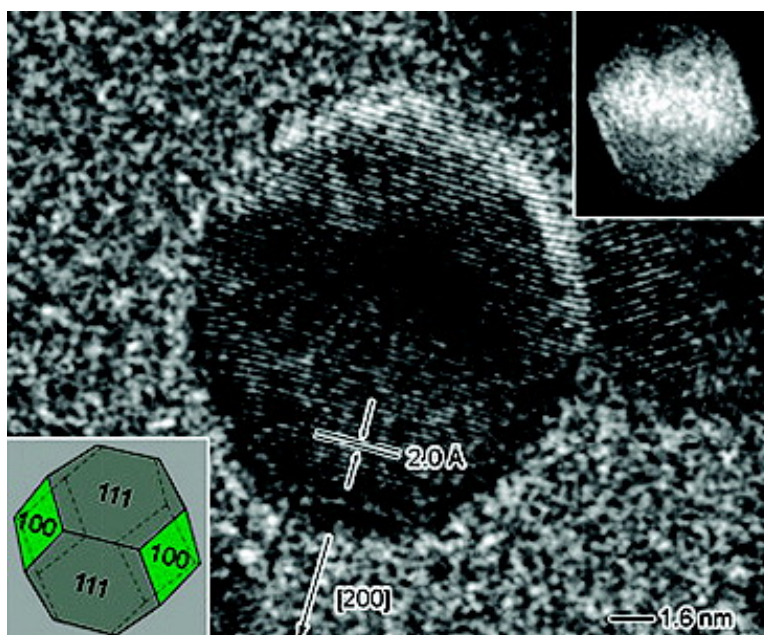


Understanding the Role of Oxidative Etching in the Polyol Synthesis of Pd Nanoparticles with Uniform Shape and Size

Yujie Xiong, Jingyi Chen, Benjamin Wiley, Younan Xia, Shaul Aloni, and Yadong Yin

J. Am. Chem. Soc., **2005**, 127 (20), 7332-7333 • DOI: 10.1021/ja0513741 • Publication Date (Web): 03 May 2005

Downloaded from <http://pubs.acs.org> on March 25, 2009



More About This Article

Additional resources and features associated with this article are available within the HTML version:

- Supporting Information
- Links to the 30 articles that cite this article, as of the time of this article download
- Access to high resolution figures
- Links to articles and content related to this article
- Copyright permission to reproduce figures and/or text from this article

[View the Full Text HTML](#)



ACS Publications
 High quality. High impact.

Understanding the Role of Oxidative Etching in the Polyol Synthesis of Pd Nanoparticles with Uniform Shape and Size

Yujie Xiong,[†] Jingyi Chen,[†] Benjamin Wiley,[‡] and Younan Xia^{*†}

Departments of Chemistry and Chemical Engineering, University of Washington, Seattle, Washington 98195-1700

Shaul Aloni and Yadong Yin

The Molecular Foundry, Lawrence Berkeley National Laboratory, Berkeley, California 94720

Received March 4, 2005; E-mail: xia@chem.washington.edu

Palladium nanoparticles serve as the primary catalyst for low-temperature reduction of pollutants emitted from automobiles¹ and organic reactions, such as Suzuki, Heck, and Stille coupling.² By tailoring the size and/or shape, one can, in principle, enhance their catalytic performance in a range of applications.³ To date, shape-controlled synthesis has been achieved for many metals and alloys, such as Co, Ag, Au, Pt, and FePt.⁴ Palladium nanoparticles of various morphologies have also been prepared in the presence of surfactants,⁵ with the mediation of RNAs,⁶ through the thermal decomposition of a Pd–surfactant complex,⁷ and via the use of a coordinating ligand.⁸ However, a more thorough understanding of the possible chemical reactions involved in the formation of Pd nanoparticles is still required in order to gain a better control over their shape, crystallinity, and yield. Here, we demonstrate that Pd cubooctahedral nanoparticles could be prepared with high yields and good uniformity using a modified polyol process, in which $[\text{PdCl}_4]^{2-}$ was reduced by ethylene glycol (EG) at 110 °C in the presence of poly(vinyl pyrrolidone) (PVP).⁹ In particular, it was found that oxidative etching of Pd nanoparticles by air might lead to the removal of twinned particles in the early stage and the dissolution of single-crystal cubooctahedra in the late stage. The key to high yields of uniform cubooctahedral nanoparticles is to utilize the former and eliminate the latter.

Figure 1 shows TEM images of Pd nanoparticles sampled at different stages from a reaction performed in air. At $t = 5$ min (Figure 1A and Figure S1A), the sample mainly contained cubooctahedra of 4–8 nm in size and 10% multiply twinned particles (MTPs). A magnified image of the 5-fold MTP is shown in the inset. As the reaction proceeded to $t = 1$ h, all the twinned particles disappeared while the average size of the cubooctahedra grew to 8 nm. In the following 2 h, there was no significant change for both size and shape. Figure 1B (also see Figure S1B) shows a typical image of the sample obtained at $t = 3$ h. During the next 2 h, the cubooctahedra were slowly dissolved until they reached an average diameter of 3 nm (Figure 1C). Beyond this point, the Pd particles began to grow again until they reached an average size of 10 nm by $t = 7$ h 40 min (Figure 1D). By analyzing the images, the size distribution of nanoparticles was found to be broader than those sampled at $t = 3$ h (Figure S2).

The cubooctahedral structure was supported by high-resolution and dark-field TEM studies (Figure 2). The fringes in the HRTEM image are separated by 2.0 Å, which agrees with the {200} lattice spacing of face-centered cubic Pd. The dark-field image (upper right inset) recorded by a {200} reflection beam unambiguously illustrates both the single crystallinity of the nanoparticle and the formation of {100} facets on its surface. The fringe orientation in

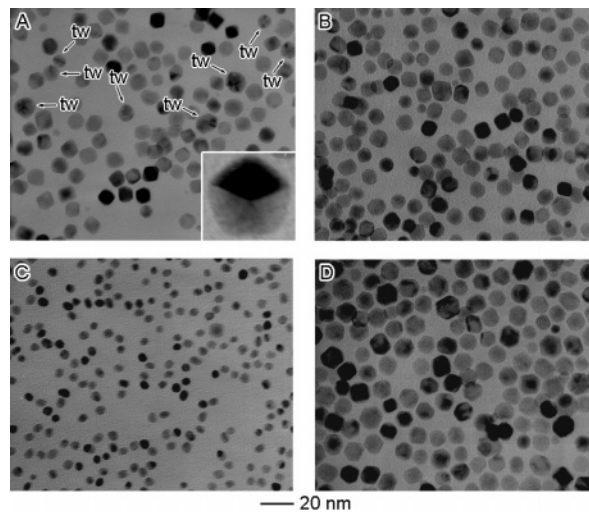


Figure 1. TEM images of Pd nanoparticles prepared in air at (A) $t = 5$ min; (B) $t = 3$ h; (C) $t = 5$ h; and (D) $t = 7$ h 40 min. Twinned particles are indicated by *tw*. The inset of (A) shows the magnified image of a 5-fold twinned nanoparticle.

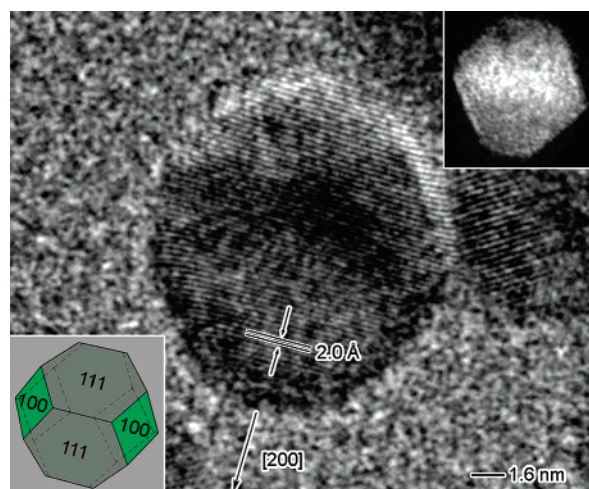


Figure 2. HRTEM image of a Pd cubooctahedron prepared in air at $t = 3$ h. The insets show the dark-field TEM image of a cubooctahedron using the {200} reflection beam (upper right) and the geometrical model of the cubooctahedron (lower left).

the HRTEM image implies that the nanoparticle is bound by 8 {111} facets and 6 {100} facets. As supported by the superior contrast in the dark-field TEM image, it can be concluded that the single-crystal nanoparticle has a cubooctahedral shape, similar to the model shown in the inset of Figure 2 (lower left). The powder X-ray diffraction (PXRD) and electron diffraction (ED) pattern

[†] Department of Chemistry.

[‡] Department of Chemical Engineering.

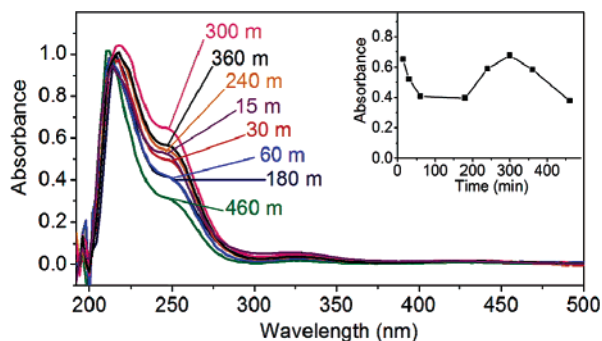


Figure 3. UV-vis spectra of solutions taken at different reaction stages. The inset depicts the time dependence of the absorbance at ~ 245 nm, which is directly proportional to the concentration of the $[\text{PdCl}_4]^{2-}$ species.

(Figure S3) also confirms the phase purity and crystallinity of the Pd cubooctahedral nanoparticles.

To appreciate the oxidative etching process, we analyzed the UV-vis spectra of the solution at different stages of the reaction (Figure 3). The absorption peaks at 245 and 327 nm can both be attributed to $[\text{PdCl}_4]^{2-}$, while the peak at 212 nm corresponds to PVP (Figure S4). The change in the concentration of $[\text{PdCl}_4]^{2-}$ could be followed by plotting the change in absorbance at ~ 245 nm against time (the inset). Similar to the case of Ag, the Cl^-/O_2 pair was responsible for the oxidative etching.¹⁰ Also, the higher reactivity of twinned Pd particles caused them to be preferentially etched in the early stage of a synthesis. They are more reactive because of the necessarily higher density of defects on their surfaces.^{11,12} Since the single-crystal cubooctahedra have fewer defects, they are relatively more stable and oxidative etching of their surfaces occurred more slowly. As a result, the twinned particles were completely dissolved by $t = 1$ h, and the size and shape of cubooctahedra remained largely unchanged between $t = 1$ h and $t = 3$ h. As the synthesis proceeded, the cubooctahedra were also etched and their size was gradually reduced. At this stage, continuous heating of EG maintained the reduction process,¹³ while etching of particles increased the concentration of $[\text{PdCl}_4]^{2-}$. Thus, after the initial dissolution stage, the reduction rate of $[\text{PdCl}_4]^{2-}$ would be increased again and the small particles could grow into larger sizes via heterogeneous nucleation. Simultaneous homogeneous nucleation during this stage might contribute to the broader size distribution. Taken together, the key to uniform Pd cubooctahedra is to limit the etching only to twinned particles and to protect the cubooctahedra from etching. For the current synthesis, the optimized time was between $t = 1$ h and $t = 3$ h.

The oxygen in air played a crucial role in the oxidative etching of Pd nanoparticles. Pd nanoparticles were not dissolved when the reaction was performed under argon (Figure S5). This observation confirms that oxidative etching was responsible for the dissolution of Pd nanoparticles. The selective removal of twinned particles via an oxidative etching process has recently been applied to the case of silver by our group.¹⁴ Without etching, silver products contained 90% twinned particles and 10% single-crystal particles. With etching, 98% of the nanoparticles became single crystals. In the present case, the etching process removed the 10% twinned particles in the sample. Twinned particles in the products prepared under argon could also be removed through an additional step of oxidative etching by exposing the sample to air for a prolonged period of time (Figure S6). If the etching time was too long, the single-crystal

cubooctahedra would start to dissolve slowly. This experiment not only proves the role of oxidative etching by Cl^-/O_2 in the dissolution of Pd nanoparticles but also demonstrates that selective etching can be used to purify and thus control the shape of nanoparticles.

In summary, uniform cubooctahedral nanoparticles of Pd were synthesized via a modified polyol process. Understanding the role of oxidative etching is critical to the achievement of both uniform shape and size. By controlling the etching process, the twinned particles in a sample could be selectively removed to leave behind uniform, single-crystal cubooctahedra. Although nanoparticles of other metals may be similarly susceptible to oxidative etching, this factor has been largely unexplored. We believe that introduction of an oxidant into the synthesis of metal nanoparticles may provide a versatile tool to control their nucleation and growth into well-defined shapes.

Acknowledgment. This work was supported in part by a DARPA-DURINT subcontract from Harvard University and a fellowship from the David and Lucile Packard Foundation. Y.X. is a Camille Dreyfus Teacher Scholar (2002). J.C. and B.W. thank the Center for Nanotechnology at the UW for a Nanotech and an IGERT fellowship (funded by NSF, DGE-9987620), respectively.

Supporting Information Available: Experimental procedure; ED and PXRD patterns of the Pd cubooctahedral nanoparticles produced in air at $t = 3$ h; UV-vis spectra of PVP and Na_2PdCl_4 in EG; TEM images of Pd nanoparticles synthesized under Ar; and geometrical illustration of twinned decahedral and icosahedral particles. This material is available free of charge via the Internet at <http://pubs.acs.org>.

References

- See, for example: (a) Fernández-García, M.; Martínez-Arias, A.; Salamanca, L. N.; Coronado, J. M.; Anderson, J. A.; Conesa, J. C.; Soria, J. *J. Catal.* **1999**, *187*, 474. (b) Nishihata, Y.; Mizuki, J.; Akao, T.; Tanaka, H.; Uenishi, M.; Kimura, M.; Okamoto, T.; Hamada, N. *Nature* **2002**, *418*, 164.
- See, for example: (a) Reetz, M. T.; Westermann, E. *Angew. Chem., Int. Ed.* **2000**, *39*, 165. (b) Kim, S.-W.; Kim, M.; Lee, W. Y.; Hyeon, T. *J. Am. Chem. Soc.* **2002**, *124*, 7642. (c) Son, S. U.; Jang, Y.; Park, J.; Na, H. B.; Park, H. M.; Yun, H. J.; Lee, J.; Hyeon, T. *J. Am. Chem. Soc.* **2004**, *126*, 5026. (d) Franzén, R. *Can. J. Chem.* **2000**, *78*, 957. (e) Li, Y.; Hong, X. M.; Collard, D. M.; El-Sayed, M. A. *Org. Lett.* **2000**, *2*, 2385.
- (a) Narayanan, R.; El-Sayed, M. A. *Nano Lett.* **2004**, *4*, 1343. (b) Vu, Y. T.; Mark, J. E. *Colloid Polym. Sci.* **2004**, *282*, 613.
- (a) Yin, Y.; Rioux, R. M.; Erdonmez, C. K.; Hughes, S.; Somorjai, G. A.; Alivisatos, A. P. *Science* **2004**, *304*, 711. (b) Chen, S.; Wang, Z. L.; Ballato, J.; Foulger, S. H.; Carroll, D. L. *J. Am. Chem. Soc.* **2003**, *125*, 16186. (c) Kim, F.; Connor, S.; Song, H.; Kuykendall, T.; Yang, P. *Angew. Chem., Int. Ed.* **2004**, *43*, 3673. (d) Sun, S.; Murray, C. B.; Weller, D.; Folks, L.; Moser, A. *Science* **2000**, *287*, 1989. (e) Jin, R.; Cao, Y. W.; Hao, E.; Metraux, G. S.; Schatz, G. C.; Mirkin, C. A. *Nature* **2003**, *425*, 487. (f) Narayanan, R.; El-Sayed, M. A. *J. Phys. Chem. B* **2004**, *108*, 5726. (g) Caswell, K. K.; Wilson, J. N.; Bunz, U. H. F.; Murphy, C. J. *J. Am. Chem. Soc.* **2003**, *125*, 13914. (h) Hao, E.; Bailey, R. C.; Schatz, G. C.; Hupp, J. T.; Li, S. *Nano Lett.* **2004**, *4*, 327.
- (a) Bradley, J. S.; Tesche, B.; Busser, W.; Maase, M.; Reetz, M. T. *J. Am. Chem. Soc.* **2000**, *122*, 4631. (b) Veisz, B.; Király, Z. *Langmuir* **2003**, *19*, 4817.
- Gugliotti, L. A.; Feldheim, D. L.; Eaton, B. E. *Science* **2004**, *304*, 850.
- Kim, S. W.; Park, J.; Jang, Y.; Chung, Y.; Hwang, S.; Hyeon, T.; Kim, Y. W. *Nano Lett.* **2003**, *3*, 1289.
- Son, S. U.; Jang, Y.; Yoon, K. Y.; Kang, E.; Hyeon, T. *Nano Lett.* **2004**, *4*, 1147.
- See Supporting Information for full experimental description.
- Cotton, F. A.; Wilkinson, G. *Advanced Inorganic Chemistry*, 5th ed.; John Wiley & Sons: New York, 1988; p 869.
- (a) Wang, Z. L. *J. Phys. Chem. B* **2000**, *104*, 1153. (b) Zhang, Y.; Doherty, M. F. *AIChE J.* **2004**, *50*, 2101.
- Gai, P. L.; Harmer, M. A. *Nano Lett.* **2002**, *2*, 771.
- Fievet, F.; Lagier, J. P.; Figlarz, M. *MRS Bull.* **1989**, 29.
- Wiley, B.; Herricks, T.; Sun, Y.; Xia, Y. *Nano Lett.* **2004**, *4*, 1733.

JA051374I